Probabilistic performance assessment of low ductility r.c. frames retrofitted by elasto-plastic dissipative braces

F. Freddi, E. Tubaldi, L. Ragni
Università Politecnica delle Marche, Ancona, Italy

A. Dall'Asta
University of Camerino, Ascoli Piceno, Italy

ABSTRACT:
This study aims at evaluating, by means of a probabilistic approach, the effectiveness of dissipative braces based on elasto-plastic devices in reducing the vulnerability of existing reinforced concrete buildings designed before the introduction of modern anti-seismic codes. A benchmark 2-dimensional reinforced concrete frame whit low ductility capacity is considered as case study. The dissipative braces are designed for different levels of the target shear capacity assigned to the bracing system, following a design method involving the pushover analysis of the bare frame. The probabilistic seismic response and vulnerability of the structure are investigated by building fragility curves of the system and of its most vulnerable components.

Keywords: Vulnerability of low ductility r.c. frames, seismic retrofit, fragility curves, elasto-plastic devices.

1. INTRODUCTION

The damage occurred during recent earthquakes in many existing reinforced concrete (r.c.) buildings designed before the introduction of modern anti-seismic codes has shown that these structures are very vulnerable to the seismic action due to their reduced ductility capacity. Therefore, the assessment and reduction of the seismic vulnerability of these systems is a task of extreme importance. Passive control systems have proven to be very efficient devices for the seismic retrofit of existing r.c. frames. Dissipation devices provide a supplemental path for the earthquake induced horizontal actions and thus enhance the seismic behaviour of the frame by adding stiffness (in some cases) and dissipation capacity to the bare frame. Among the various types of dissipative devices currently applied in the retrofit of existing structures (Soong and Spencer 2002, Christopoulos and Filiatrault 2006), those with elasto-plastic behaviour appear to be very promising due to the large hysteresis cycles they can undergo during the earthquake action.

The introduction of an elasto-plastic bracing system into a low ductility frame usually induces remarkable changes both in the collapse modalities and in the probabilistic properties of the seismic behaviour of the structure. In particular, the latter aspect assumes a considerable importance in consequence of the high degree of uncertainty affecting the seismic input and of the differences in the propagation of this uncertainty through the two resisting systems (frame and dissipative bracing) arranged in parallel. Thus, the knowledge of the probabilistic properties of the seismic response and the assessment of the vulnerability of the system before and after the retrofit is a crucial task in defining reliable design procedures for the dissipative braces. Usually, the vulnerability assessment involves the use of seismic fragility curves. These probabilistic tools provide the probability that a specified limit state or failure condition is exceeded, conditional to the strong-motion shaking severity, measured by means of an appropriately selected intensity measure (*IM*). Some recent studies have been developed which employ fragility curves in evaluating the effects of various techniques for retrofitting both frames and bridges. In particular, Hueste and Bai (2007) investigated the effectiveness of different retrofit techniques in reducing the seismic fragility of a typical 1980s RC building in Central US. Ramamoorthy et al. (2006) assessed the seismic vulnerability of a two-story reinforced concrete frame building designed for gravity loads only. They also developed fragility curves for the

same building retrofitted by means of column strengthening, showing the effectiveness of this technique in reducing the frame vulnerability. Padgett and DesRoches (2008) investigated the impact of different retrofit measures on the vulnerability of multiple components of multi-span continuous bridges. Kim and Shinozuka (2004) performed a Monte Carlo simulation to study the seismic vulnerability of two sample bridges in California before and after retrofit.

In this paper, the authors consider the case of r.c. frames with limited ductility whose seismic performance is enhanced by adding, within its bays, a system of diagonal dissipative braces with elasto-plastic behaviour. Obviously, the seismic response of the retrofitted system depends on the criteria adopted for the brace dimensioning. Usually, the stiffness distribution of the dissipative braces at each storey are designed so that the first vibration mode of the bare frame remains unvaried after the retrofit. This permits to avoid drastical changes to the distribution of the frame internal actions, at least in the range of the elastic frame behaviour. Moreover, in order to obtain a simultaneous yielding of the devices at all the storeys, their strength distribution is assumed proportional to the distribution of the storey shear of the bare frame relative to the first vibration mode. This design approach, already followed by many authors (Braga and D'Anzi 1994, Kasai et al. 1998, Mazza and Vulcano 2008, Dall'Asta et al. 2009), is employed in this study for the retrofit of a benchmark r.c. frame (Bracci et al. 1992) designed for gravity loads only, by considering different levels of the shear capacity of the dissipative system. Fragility curves for the system before and after the retrofit are built through incremental non linear dynamic analysis for a set of different ground motion (g.m.) records. In particular, in addition to global system fragility curves, component fragility curves are built for single structural members (e.g., beam, column, brace or group of these elements) in order to highlight the most vulnerable elements before ad after the retrofit.

2. RETROFITTING OF R.C. FRAME WITH ELASTO-PLASTIC BRACES

The design procedure, synthetically illustrated below, can be applied to the design of dissipative braces exhibiting an elasto-plastic behaviour. The interested reader is referred to Dall'Asta et al. (2009) for a more detailed description. The dissipative braces considered in this paper are made by an elasto-plastic dissipation device placed in series with an elastic brace exhibiting adequate overstrength. The properties of the dissipative brace can be defined based on the properties of its components. In particular, if K_b denotes the axial stiffness of the elastic brace and K_0, F_0 and μ_{0u} respectively the stiffness, yielding force and ductility capacity of the elasto-plastic device, the dissipative brace stiffness K_d and ductility capacity μ_{du} are given by the following relations:

$$K_d = \frac{K_b K_0}{K_b + K_0} \quad \text{and} \quad \mu_{du} = \frac{K_0 + K_b \mu_{0u}}{K_b + K_0} \tag{2.1}$$

while the yielding force F_d is equal to F_0. Usually, the value of μ_{0u} is in the range 15-20 while the value of μ_{du} is in the range 10-15, depending on the ratio K_0/K_b. The method followed for designing the dissipative system is based on pushover analysis of the existing frame under a distribution of forces corresponding to its first vibration mode, in order to assess its capacity. The "collapse point" for the frame is defined by the values of the maximum displacement at the top floor d_u and by the maximum base shear V_f^1 the frame is capable to withstand. The dissipative bracing system is assumed to behave as an elastic-perfectly plastic system, with shear capacity equal to V_d^1, ductility capacity equal to μ_{du} and with the same collapse displacement of the bare frame (d_u). This last assumption aims at obtaining a simultaneous failure of both the frame and the dissipative braces. It is noteworthy that the value of V_d^1 is a design choice and depends on the objective of the retrofit. For a given value of V_d^1, the stiffness of the bracing system at the first storey is obtained as:

$$K_d^1 = \frac{V_d^1 \mu_{du}}{d_u \delta^1} \tag{2.2}$$

where δ^1 is the inter-storey drift at the first storey, normalized with respect to the top floor displacement according to the first modal shape. The shear V_d^i and stiffness K_d^i of the dissipating bracing system at each storey can be determined through the following relations:

$$V_d^i = V_d^1 v^i \quad \text{and} \quad K_d^i = K_d^1 k^i \tag{2.3}$$

where v^i and k^i are the shear force and stiffness at each storey, normalized with respect to the base shear and base stiffness according to the first mode of the bare frame. By this way, the stiffness distribution of the dissipative braces at each storey ensures that the first modal shape of the bare frame remains unvaried after the retrofit. This avoids drastical changes to the internal action distribution in the frame, at least in the range of the elastic behaviour. Additionally, the chosen strength distribution of the dissipative braces aims at obtaining simultaneous yielding of the devices at all the storeys and, thus, a global ductility of the bracing system coinciding with the ductility of the single braces. Given V_d^i and K_d^i, the braces properties (K_0^i, F_0^i and K_b^i) at each storey can be determined based on the number of braces at each storey and on geometrical considerations.

3. PROBABILISTIC METHODOLOGY FOR SYSTEM VULNERABILITY ASSESSMENT

The evaluation of the performance of the frame before and after retrofit requires a probabilistic approach due to the high degree of uncertainty characterizing the earthquake input and the system properties. The earthquake input motion is usually characterized by a degree of uncertainty that overcomes the aleatoric uncertainty in material and geometrical system properties. Thus, only the former source of uncertainty is considered in this study by selecting a set of natural g.m. records which reflect the variability in duration, frequency content, and other characteristic of the earthquake input which is likely to act on the system. The selected records are compatible with a input uniform hazard spectrum, thus they are characterized by a given intensity and they can be assigned an annual frequency of occurrence, depending on the site. In order to evaluate the system performance for other seismic intensity values and, thus, to generate fragility curves, incremental dynamic analysis (IDA) is performed by subjecting the system to the selected natural records for increasing values of the seismic intensity. In this study, the spectral acceleration at the fundamental period of the structure $S_a(T)$ is used as seismic intensity measure *IM* (Katsanos et al. 2009). This choice requires the normalization of the spectrum-compatible records in order to obtain the same value of $S_a(T)$ for the natural period of the structure T, which is different for the bare frame and the retrofitted frame. The results of IDA are multi-record IDA curves, i.e., the plot of appropriately selected engineering demand parameters (EDPs) monitoring the system response vs *IM*. The EDPs chosen in the present study are *a)* the maximum-over-time values of the axial concrete strain ε_c and steel strain ε_s, at each element, *b)* the maximum-over-time values of each element's shear force and *c)* the ductility demand at each dissipative brace μ_d. The maximum interstory drift, often employed in other studies (Kwon and Elnashai 2006, Hueste and Bai 2007), is not considered here as EDP since it would not be able to capture the modifications to the frame response and capacity induced by the introduction of the bracing system, (e.g., the axial load at the columns connected to the braces significantly varies after the retrofit). Consequently, the limit states considered in developing the fragility curves are: *LS1)* ε_c exceeding the limit ε_{cu} at any element, *LS2)* ε_s exceeding the limit ε_{su} at any element, *LS3)* the shear demand at any column exceeding the shear resistance and *LS4)* the ductility demand of the dissipative braces μ_d overcoming the ductility capacity μ_{du} at any storey. Based on IDA results, system fragility curves are built for the bare and for the retrofitted frame assuming a series arrangement of the failure modes (i.e., failure in one mode yields system failure). The fragility curves are also synthetically described by means of two parameters: the median *IM* at collapse $\widehat{IM}_c$, i.e. the *IM* which corresponds to 50% probability of failure, and the dispersion β_c, defined by the following expression:

$$\beta_c = \frac{1}{2}\ln\left(\frac{IM_{c,84}}{IM_{c,16}}\right) \tag{3.1}$$

where $IM_{c,84}$ and $IM_{c,16}$ are the *IM* values corresponding to the 84th and the 16th fractiles of the fragility curve, i.e., the values of the *IM* which yield failure respectively in 84 and 16 cases over 100. These two parameters are used to compare the performance of the bare and of the retrofitted frame and, thus, to assess the effectiveness of the dissipative braces system, designed according to the above described method, in reducing the vulnerability of the frame. In particular, the first parameter, $\widehat{IM}_c$, divided by the value $S_a(T)$ of the code spectrum at the system natural period *T*, provides the so called "collapse margin ratio" m_{50} (Liel et al. 2010), i.e., the factor the input spectrum has to be scaled by in order to induce system collapse in 50% of the cases. It is noteworthy that this normalized measure allows to account for the change in the seismic input (spectral) intensity due to the variation in the natural period of the system. Typically, the introduction of the dissipative braces leads to an increase of the factor m_{50} with respect to the bare frame. In a similar way, based on the ratio $IM_{c,16}/\ S_a(T)$ (or $IM_{c,84}/\ S_a(T)$) one can define the factor m_{16} (m_{84}) as the factor the natural records have to be scaled by in order to induce system collapse in 16% (84%) of the cases. The factors m_{16} and m_{84} permit to estimate the effectiveness of the retrofit in reducing the frame seismic vulnerability with higher and lower confidence with respect to m_{50}. In addition to system fragility curves, component fragility curves are built for single structural members (e.g., beam, column, dissipative brace or group of these elements) in order to highlight the most vulnerable elements. These curves provide a way to assess the efficiency of the design procedure, whose objective is to obtain a simultaneous failure of both the frame and the braces or, in probabilistic terms, the same vulnerability of the frame and of the bracing system (i.e., an equal probability of failure given an *IM* value).

4. APPLICATION TO A CASE STUDY

The probabilistic methodology illustrated above is applied to the vulnerability assessment of a 2-dimensional frame belonging to a r.c. building whose seismic response has already been investigated in other studies (Bracci et al. 1992, Kwon and Elnashai 2006). The building has been designed for gravity loads only and without any seismic detailing, simulating the design before to the introduction of modern anti-seismic codes. The frame consists of three stories 3.66 m high for a total height of 11 m and three bays, each 5.49 m wide. Columns have a 30×30 cm^2 square section while beams are 23×46 cm^2 at each floor. Reinforcement bars are made of Grade 40 steel (mean yield strength f_y = 337 MPa) while concrete has a mean compressive strength f_c = 33.6 MPa. Fig. 4.1a) contains the general layout of the structure and Fig. 4.1b) shows some beam reinforcement detailing. The interested reader is referred to Bracci et al. (1992) for additional detailing. The limits to concrete ε_{cu} and steel ε_{su} strain capacity are respectively and conventionally set to 0.0035 and 0.04. The shear capacity of each column is evaluated according to Priestley et al. (1994) formula. The structural finite element model of the frame, built within OpenSees (McKenna et al. 2006), employs beam with hinges elements (Scott and Fenves 2006) to model the hysteretic behaviour of beams and columns. The plastic hinge length for both beam and column has been evaluated based on the formula proposed in Panagiotakos and Fardis (2001):

$$L_p = 0.12L_V + 0.014\alpha d_{bL} f_y \tag{4.1}$$

where L_V is the element shear length, α is a parameter which assumes the value 0 (or 1) in presence (absence) of lap-spliced rebars at the element's end sections, d_{bL} is the longitudinal bar diameter and f_y is the steel yield strength. The elastic part of each element is assigned an effective flexural stiffness value, evaluated through moment-curvature analysis, for the axial force level induced by the dead loads. The rigid-floor diaphragm is modelled by assigning an high value to the axial stiffness of the beams. The accuracy of the finite element model has been checked through comparison with the results of numerical and experimental investigations performed by other authors (Bracci et al. 1992, Kwon and Elnashai 2006).

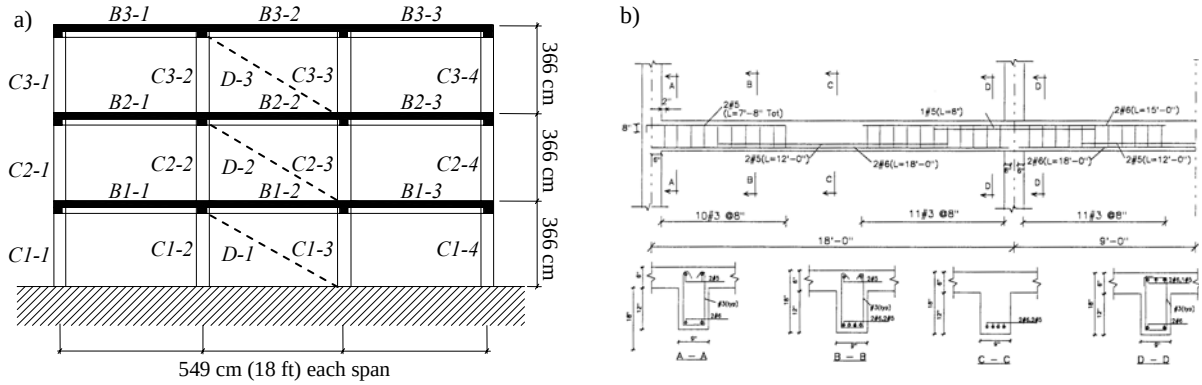

Figure 4.1.a) General layout of the structure and braces arrangement, b) beam reinforcement detailing.

In Fig. 4.2a) the pushover curve obtained for the load distribution relative to the first vibration mode of the bare frame (mass participation factor of 86.4%) is shown and the limit corresponding to the failure of the beam *B1-3* of Fig. 4.1a), which occurs first, is posed in evidence. This limit, which is attained for an inter-storey drift of about 1.5%, is due to concrete failure ($\varepsilon_c=\varepsilon_{cu}$) and corresponds to a displacement d_u of 0.124 m and a shear capacity V_f^1 of 147 kN. It is observed that the frame ductility capacity corresponding to the chosen strain capacity is very limited.

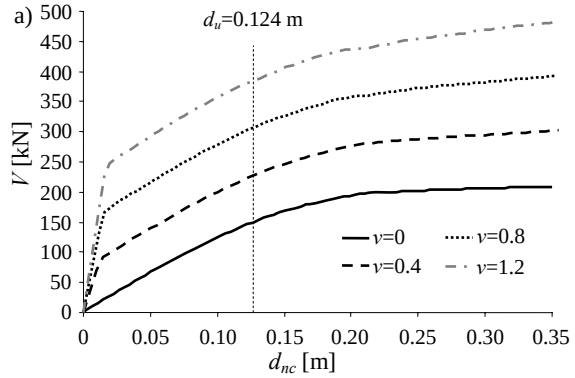

b)

	v=0.4		v=0.8		v=1.2	
Storey	F_d^i	k_d^i	F_d^i	k_d^i	F_d^i	k_d^i
	[kN]	[kN/m]	[kN]	[kN/m]	[kN]	[kN/m]
1	87	29920	174	59841	260	89761
2	74	21241	149	42481	223	63722
3	43	19271	85	38542	128	57813

Figure 4.2.a) Pushover curves of the bare and retrofitted frame and b) brace properties at each storey.

The bare frame is retrofitted by inserting a bracing system designed for three values of the ratio v between the shear capacity of the bracing system V_d^1 and that of the frame V_f^1, i.e., 0.4, 0.8, 1.2. The ductility capacity assumed for the dissipative bracing system is μ_{du} = 12. The dissipative devices considered in this study are Buckling-Restrained Axial Dampers (BRADs) (Antonucci et al. 2007) made of an internal steel core whose buckling is prevented by an external steel casing filled with mortar. These devices are usually short, so that they are able to yield for small displacements and thus can be used in the retrofit of r.c. frames with limited ductility collapsing for small lateral displacements. The maximum ductility capacity of this kind of devices is about μ_{0u} = 15 and, in the design procedure, the value μ_{du} = 12 is assumed for the dissipative braces. This leads to elastic braces which are not excessively stiff but at the same time adequate to avoid buckling. The pushover curves of the retrofitted frame for the different levels of v are shown in Fig. 4.2a) while the braces properties are shown in Fig. 4.2b). For the purpose of developing fragility curves, a number of 14 natural g.m. records are selected from the European database (Ambraseys et al. 2000). These records are compatible with the Eurocode 8–type 1 (ECS 2005) soil type D response spectrum with a peak ground acceleration PGA=0.1*g*. They have been chosen in a range of magnitude and source to site distance of 5.5-7 and 25-75 respectively. Fig. 4.3a) compares the spectra of each g.m. record, the mean spectrum and the code spectrum. Fig. 4.3b) shows the spectra of the records after normalization with respect to the natural period of vibration of the bare frame (T_1=1.336 s). It is noteworthy that the vibration period of the retrofitted frame for the different values of v are different. They are: $T_1(v=0.4)$=0.779 s,

$T_1(\nu=0.8)=0.617$ s, and $T_1(\nu=1.2)=0.533$ s.

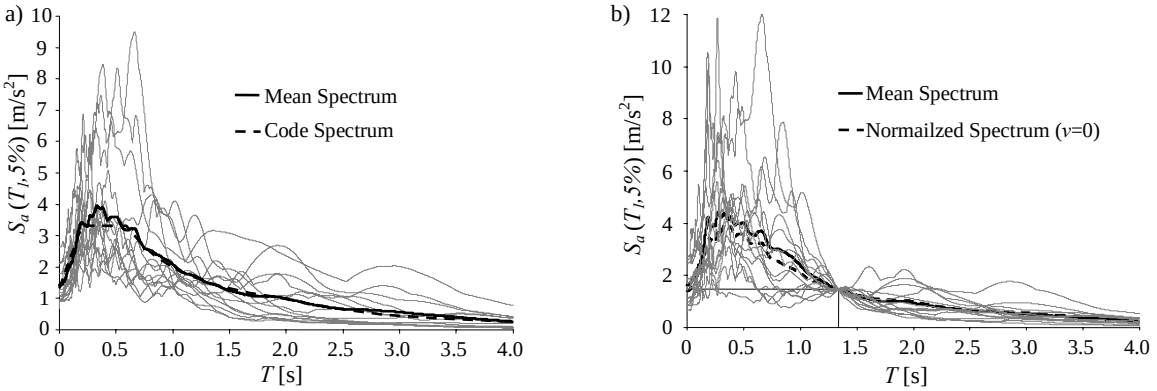

Figure 4.3.a) Record spectra, mean spectrum and code spectrum and b) mean spectrum vs. normalized mean spectrum for the bare frame.

Fig. 4.4a) shows the system fragility curve of the bare frame accounting for concrete failure, steel failure and shear failure. In general concrete failure (*LS1*) is most likely to occur, steel failure (*LS2*) is probable for beams only and shear failure (*LS3*) is very rare. In the same figure, component fragility curves of the most vulnerable elements of the frame (beam *B1-3* and column *C1-3*) are reported at which *LS1* failure is prevailing. It is noteworthy that their contribution to the system fragility is very significant. In Fig. 4.4b) the maximum deformation demands at these elements, in terms of concrete strain, are shown for all the records considered, together with the median value (50th fractile), the 84th and the 16th fractile. The dispersion of the seismic response is quite significant for all the structural components as a consequence of the limited efficiency of the selected *IM* (Katsanos et al. 2009). However, it can also observed that the dispersion at the column is significantly higher than that at the beam due to the strong variation of the axial force during the seismic event.

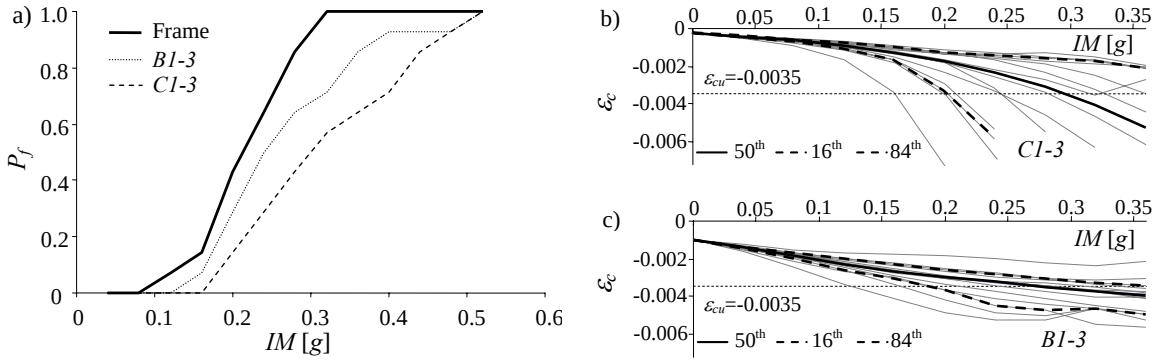

Figure 4.4.a) Bare frame fragility curves $P_f(IM)$ for the system and the most vulnerable resisting elements, b) concrete strain demand at column *C1-3* and c) concrete strain demand at beam *B1-3*.

Fig. 4.5a) shows the system fragility curves for the bare frame and the system retrofitted for the three different levels of ν. Globally, an increase in the value of $\widehat{IM}_c$ is observed for the increasing values of ν, as expected. In order to highlight the effectiveness of the retrofit in increasing the seismic performance considering different levels of confidence, the collapse margin ratios corresponding to the 84th , the 50th and the 16th fractile are reported in Fig. 4.5b) for increasing values of ν. In Fig. 4.5c) the dispersion measure β_c is reported. It can be observed that the value of β_c for all the cases of retrofit is larger than the corresponding value of the bare frame, due to the more pronounced nonlinear behaviour induced by the dissipative braces, characterized by an almost elastic-perfectly plastic response. However, for high ν values, the dispersion measure β_c decreases. This effect can be explained by observing that the system fragility reflects the fragility of the most vulnerable components of the system.

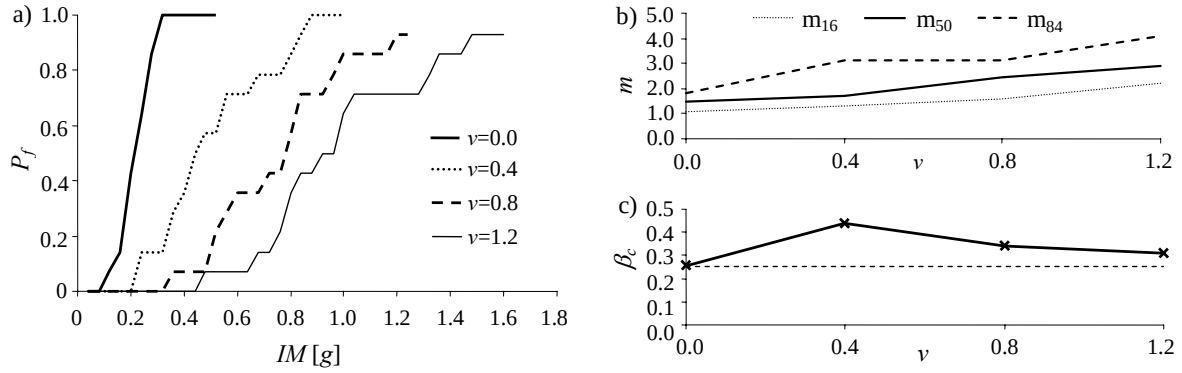

Figure 4.5.a) System fragility curves for the bare frame and for the three different retrofitted systems, b) variation of collapse margin ratios with v, c) variation of dispersion of IM at collapse (β_c)with v.

The component fragility curves are shown in Fig. 4.6a) for the extreme cases corresponding to v=0.4 and v=1.2. For v = 0.4 the system fragility almost coincides with the fragility of the dissipative brace at the third storey. This means that in most of the cases the system failure occurs due to the localization of the ductility demand at the brace of the last storey (*D-3*). This element is characterized by an highly dispersed response, as shown in Fig. 4.6b). On the other hand, for v = 1.2, the fragility curves of dissipative braces at the three storeys are very similar and significantly far from the global system fragility. Beam *B1-3* is the most vulnerable element, characterized by a dispersion of ε_c which is significantly lower than the dispersion of the ductility demand μ_d of the dissipative braces, as shown in Fig. 4.6c). It is important to notice that, in both the cases, the frame and the dissipative braces are not characterized by the same vulnerability, as sought in the design. This design objective is very difficult to achieve as a consequence of the assumptions made in the design procedure and of the different dispersion which characterizes the components response.

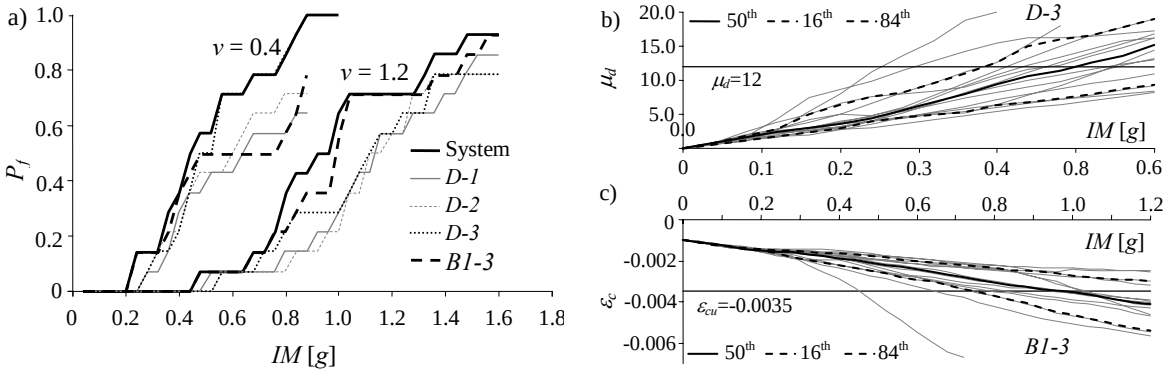

Figure 4.6.a) System and components fragility curves for v=0.4 and v=1.2, b) ductility demand at the dissipative braces *D-3* for v=0.4 and c) concrete strain demand at beam *B1-3* for v=1.2.

5. CONCLUSION

The study analyzes, with a probabilistic approach, the seismic performance of existing reinforced concrete buildings with limited ductility, retrofitted by means of dissipative braces based on elasto-plastic devices. A benchmark 2-dimensional frame representative of the analyzed class of buildings is considered and retrofitted for different values of the shear capacity of the bracing system. The method followed for designing the dissipative system is based on the first vibration mode of the response of the bare frame, which remains unvaried after retrofit. Fragility curves of the frame before and after the retrofit are generated based on incremental non linear dynamic analysis, by considering a set of input ground motion which reflect the randomness of the earthquake excitation. In addition to global system fragility curves, component fragility curves are built for single structural components. The obtained results show that, for all the cases of retrofit, the collapse margin ratio increases for increasing values

of ν and the dispersion of the seismic response is always higher than in the case of the bare frame, due to the more pronounced nonlinear behaviour induced by the dissipative bracing system. However, it is observed that the dispersion of the response varies with *v* due to the change in the most vulnerable components of the system. Although the design objective is to achieve comparable vulnerabilities for the frame and the dissipative braces, this does not always occur in the discussed cases. This may be ascribed to both the assumptions made in the design procedure and to the different uncertainty which characterizes the response of the various components.

REFERENCES

Ambraseys, N., Smith, P., Berardi, R., Rinaldis, D., Cotton, F. and Berge-Thierry, C. (2000). Dissemination of European Strong-Motion Data. CD-ROM Collection. European Council, Environment and Climate Research Programme.

Antonucci, R., Cappanera, F., Balducci, F., Castellano, M.G. (2007). Adeguamento sismico del Liceo classico "Perticari" di Senigallia (AN). *XII Convegno Nazionale ANIDIS: L'Ingegneria sismica in Italia*, Pisa, Italy.

Bracci, J.M., Reinhorn, A.M., Mander, J.B. (1992). Seismic resistance of reinforced concrete frame structures designed only for gravity loads: part I-design and properties of a one-third scale model structure. Technical report NCEER-92-0027.

Braga, F. and D'Anzi, P. (1994). Steel braces with energy absorbing devices: a design method to retrofit reinforced concrete existing buildings. *Italian-French symposium: Strengthening and repair of structures in seismic area* Nice, France, 146-154.

Christopoulos, C. and Filiatrault, A. (2006). Principles of passive supplemental damping and seismic isolation. IUSS Press, Pavia, Italy.

Dall'Asta, A., Ragni, L., Tubaldi, E., Freddi, F. (2009). Design methods for existing r.c. frames equipped with elasto-plastic or viscoelastic dissipative braces, *XIII Convegno Nazionale ANIDIS: L'Ingegneria sismica in Italia*, Bologna, Italy.

European Committee for Standardization (ECS) (2005). Eurocode 8 - Design of structures for earthquake resistance, EN1998, Brussels.

Hueste, M.D. and Bai, J.W. (2007). Seismic Retrofit of a Reinforced Concrete Flat-Slab Structure: Part II - Seismic Fragility Analysis. *Engineering Structures* **29:6**,1178-1188.

Kasai, K., Fu, Y. and Watanabe, A. (1998). Passive control systems for seismic damage mitigation. *Journal of Structural Engineering* **124:5**,501-512.

Katsanos, E.I., Sextos, A.G. and Manolis, G.D. (2009). Selection of earthquake ground motion records: A state-of-the-art review from a structural engineering perspective. *Soil Dynamics and Earthquake Engineering* **30:4**,157-169.

Kim, S.H. and Shinozuka, M. (2004). Development of fragility curves of bridges retrofitted by column jacketing. *Probabilistic Engineering Mechanics* **19:1-2**,105-112.

Kwon, O.S. and Elnashai, A. (2006). The effect of material and ground motion uncertainty on the seismic vulnerability curves of RC structure. *Engineering Structures* **28:2**,289–303.

Liel, A.B., Haselton, C.B. and Deierlein, G.G. (2010). Seismic Collapse Safety of Reinforced Concrete Buildings: II. Comparative Assessment of Non-Ductile and Ductile Moment Frames, *Journal of Structural Engineering* (accepted for publication).

Mazza, F. and Vulcano, A. (2008). Displacement-based design of dissipative braces at a given performance level of a framed building. *14th World Conference on Earthquake Engineering*, Beijing, China.

McKenna, F., Fenves, G.L., Scott, M.H. (2006). OpenSees: Open system for earthquake engineering simulation. Pacific Earthquake Engineering Center, University of California, Berkeley, CA.

Padgett, J.E. and DesRoches, R. (2008). Methodology for the Development of Analytical Fragility Curves for Retrofitted Bridges. *Journal of Earthquake Engineering and Structural Dynamics* **37:8**,1157-1174.

Panagiotakos, T.B., Fardis, M.N. (2001). Deformation of reinforced concrete members at yielding and ultimate. *ACI Structural Journal* **98:2**,135-148.

Priestley, M.J.N., Verma, R. and Xiao, Y. (1994). “Seismic shear strength of reinforced concrete columns.” *Journal of Structural Engineering* **120:8**, 2310-2329.

Ramamoorthy, S., Gardoni, P. and Bracci, J. (2006). Seismic Fragility estimates for Reinforced Concrete Framed Buildings. Technical Report, Center for Design and Construction Integration, Texas A&M University.

Scott, M.H. and Fenves, G.L. (2006). Plastic hinge integration methods for force-based beam-column elements. *Journal of Structural Engineering* **132:2**,244-252.

Soong, T.T. and Spencer, B.F. (2002). Supplemental energy dissipation: state-of-the-art and state-of-the-practice. *Engineering Structures* **24:3**,243-259.